# E4F1 controls a transcriptional program essential for pyruvate dehydrogenase activity

Matthieu Lacroix, Geneviève Rodier, Olivier Kirsh, Thibault Houles, Hélène Delpech, Berfin Seyran, Laurie Gayte, François Casas, Laurence Pessemesse, Maud Heuillet, et al.

# E4F1 controls a transcriptional program essential for pyruvate dehydrogenase activity

Matthieu Lacroix[a,b,c,d,e,1], Geneviève Rodier[a,b,c,d,e,f,1], Olivier Kirsh[f,g,1], Thibault Houles[a,b,c,d,e,f,2], Hélène Delpech[a,b,c,d,e,f,2], Berfin Seyran[a,b,c,d,e], Laurie Gayte[a,b,c,d,e], Francois Casas[c,h], Laurence Pessemesse[c,h], Maud Heuillet[i,j,k], Floriant Bellvert[i,j,k], Jean-Charles Portais[i,j,k], Charlene Berthet[a,b,c,d,l], Florence Bernex[a,b,c,d,l], Michele Brivet[m], Audrey Boutron[m], Laurent Le Cam[a,b,c,d,e,3,4], and Claude Sardet[a,b,c,d,e,f,3,4]

[a]Institut de Recherche en Cancérologie de Montpellier, Montpellier F-34298, France; [b]INSERM, U1194, Montpellier F-34298, France; [c]Université Montpellier, Montpellier F-34090, France; [d]Institut du Cancer Montpellier, Montpellier F-34298, France; [e]Equipe labellisée Ligue Contre le Cancer, 75013 Paris, France; [f]Institut de Génétique Moléculaire de Montpellier, UMR5535, CNRS, Montpellier F-34293, France; [g]CNRS, UMR7216, Epigenetics and Cell Fate, University Paris Diderot, Sorbonne Paris Cite, 75013 Paris, France; [h]Dynamique Musculaire et Métabolisme, Institut National de la Recherche Agronomique, UMR866, F-34060 Montpellier, France; [i]Université de Toulouse, Institut National des Sciences Appliquées, Université Paul Sabatié, Institut National Polytechnique, F-31077 Toulouse, France; [j]UMR792 Ingénierie des Systèmes Biologiques et des Procédés, Institut National de la Recherche Agronomique, F-31400 Toulouse, France; [k]CNRS, UMR5504, F-31400 Toulouse, France; [l]Montpellier Network of Experimental Histology, BioCampus, CNRS, UMS3426, F-34094 Montpellier, France; and [m]Department of Biochemistry, Bicêtre Hospital, 94270 Le Kremlin Bicetre, France

Edited by Steven L. McKnight, The University of Texas Southwestern Medical Center, Dallas, TX, and approved August 9, 2016 (received for review February 18, 2016)

**The mitochondrial pyruvate dehydrogenase (PDH) complex (PDC) acts as a central metabolic node that mediates pyruvate oxidation and fuels the tricarboxylic acid cycle to meet energy demand. Here, we reveal another level of regulation of the pyruvate oxidation pathway in mammals implicating the E4 transcription factor 1 (E4F1). E4F1 controls a set of four genes [dihydrolipoamide acetlytransferase (*Dlat*), dihydrolipoyl dehydrogenase (*Dld*), mitochondrial pyruvate carrier 1 (*Mpc1*), and solute carrier family 25 member 19 (*Slc25a19*)] involved in pyruvate oxidation and reported to be individually mutated in human metabolic syndromes. E4F1 dysfunction results in 80% decrease of PDH activity and alterations of pyruvate metabolism. Genetic inactivation of murine *E4f1* in striated muscles results in viable animals that show low muscle PDH activity, severe endurance defects, and chronic lactic acidemia, recapitulating some clinical symptoms described in PDC-deficient patients. These phenotypes were attenuated by pharmacological stimulation of PDH or by a ketogenic diet, two treatments used for PDH deficiencies. Taken together, these data identify E4F1 as a master regulator of the PDC.**

E4F1 | PDH | pyruvate | muscle | endurance

The pyruvate dehydrogenase (PDH) complex (PDC) is a mitochondrial multimeric complex that catalyzes the oxidative decarboxylation of pyruvate into acetyl-CoA (AcCoA), thus linking pyruvate metabolism to the tricarboxylic acid (TCA) cycle. Localized in the mitochondrial matrix, the core PDC is composed of multiple copies of three catalytic enzymes: PDHA1/E1, dihydrolipoamide transacetylase (DLAT)/E2, and dihydrolipoamide dehydrogenase (DLD)/E3 (1). To fuel the PDC, pyruvate translocates across the inner mitochondrial membrane through the heterodimeric pyruvate transporter mitochondrial pyruvate carrier 1 (MPC1)/MPC2 (2, 3). The activity of the PDC depends on several cofactors, including lipoate, CoEnzymeA (CoA), FAD+, NAD+, and thiamine pyrophosphate, the latter being imported in the mitochondria by the SLC25A19 transporter (4). So far, fine-tuning of PDC activity has been mainly attributed to post-translational modifications of its subunits (5, 6), including the extensively studied phosphorylation of PDHA1/E1 modulated by PDH kinases (PDK1–4) and phosphatases (PDP1–2). However, in lower organisms, such as *Escherichia coli* and *Candida albicans*, PDC is also controlled at the transcriptional level by the coordinated regulation of genes encoding its components and regulators (7, 8). The importance of such transcriptional regulation of the PDC in mammals remains elusive. Physiological regulation of PDC plays a pivotal role in metabolic flexibility to adjust energetic metabolism and biosynthesis to nutrient availability and energy demand (9), such as in skeletal muscles during exercise (10). PDH activity is altered in several human metabolic syndromes associated with chronic lactate acidosis, progressive neurological degeneration, and muscular atonia (11). Genetic mitochondrial disorders associated with PDH deficiency mainly result from hypomorphic mutations in genes encoding subunits or regulators of the PDC, including in *PDHA1*, *DLAT*, *DLD*, *PDP1*, *MCP1*, and *SLC25A19* (3, 11–13). The diverse clinical manifestations of PDC-deficient patients are significantly, but only partly, improved by ketogenic diets that provide alternative energetic substrates or by treatment with PDK inhibitors, such as dicholoroacetate (DCA). Thiamine/lipoic acid supplementations that favor optimal PDH activity, or bicarbonate treatment that buffers lactate acidosis, have also been tested, although with moderate efficiency (14, 15). The design of new and more efficient therapeutic approaches will require a better understanding of PDH regulation and the development of clinically relevant animal models.

Here we reveal another level of regulation of the pyruvate oxidation pathway in mammals that implicates the E4 transcription factor

## Significance

**Pyruvate dehydrogenase (PDH) deficiency is the cause of several human metabolic diseases. In mammals, the transcriptional control of PDH complex components and its impact on pathophysiology remain poorly understood. We show that E4 transcription factor 1 (E4F1) controls a transcriptional program essential for PDH activity that involves genes linked to human metabolic syndromes. Genetic inactivation of murine *E4f1* results in a strong decrease of PDH activity and severe perturbations of pyruvate metabolism. In concordance with the work of Legati et al., we show that striated muscle-specific *E4f1* KO animals display phenotypes that recapitulate these clinical symptoms, providing an exciting clinical perspective to the present work.**

Author contributions: M.L., G.R., O.K., F.C., M.B., A.B., L.L.C., and C.S. designed research; M.L., G.R., O.K., T.H., H.D., B.S., L.G., L.P., M.H., F. Bellvert, and C.B. performed research; M.L., G.R., O.K., J.-C.P., F. Bernex, L.L.C., and C.S. analyzed data; and L.L.C. and C.S. wrote the paper.

The authors declare no conflict of interest.

This article is a PNAS Direct Submission.

[1]M.L., G.R., and O.K. contributed equally to this work.

[2]T.H., and H.D. contributed equally to this work.

[3]L.L.C., and C.S. contributed equally to this work.

[4]To whom correspondence may be addressed. Email: laurent.lecam@inserm.fr or claude.sardet@inserm.fr.

This article contains supporting information online at www.pnas.org/lookup/suppl/doi:10.1073/pnas.1602754113/-/DCSupplemental.

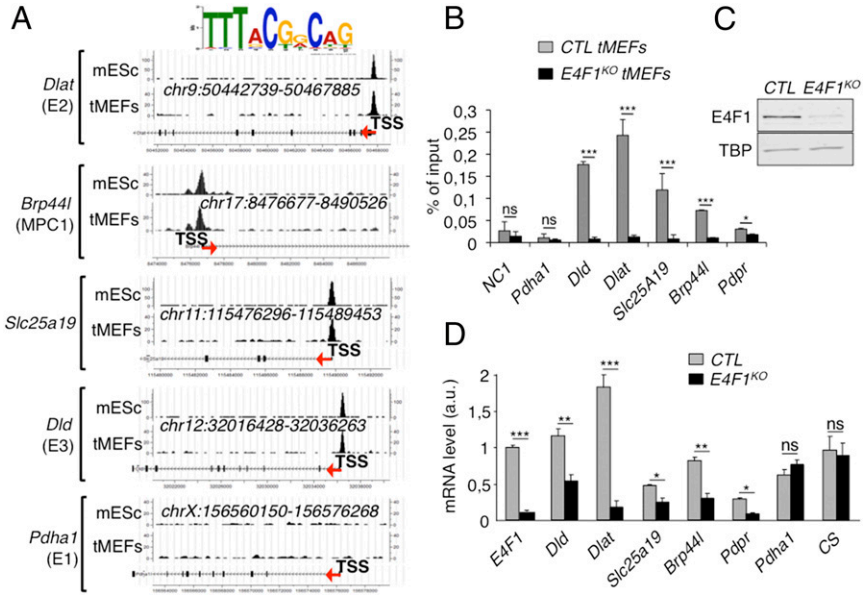


**Fig. 1.** E4F1 directly controls a transcriptional program involved in PDH activity in mammals. (*A*) E4F1 ChIP-Seq read densities in tMEFs and mouse ES cells (mES) at the *Dlat*, *Dld*, *Mpc1*/*Brp44l*, *Slc25a19*/*DNC* (deoxynucleotide carrier) genes, and at the *Pdha1* gene as a representative control locus to which E4F1 does not bind. The E4F1 consensus motif determined by MEME is shown and arrows indicate the genes orientation. (*B*) Validation of these E4F1 target genes by ChIP-qPCR assays performed in *E4f1*$^{KO}$ and control (CTR) tMEFs, 3 d after transduction with a self-excising Cre-retrovirus. A gene-poor noncoding region of chromosome 8 (NC1) and the *Pdha1* promoter region (TSS) were used as controls. Enrichments are represented as percentages of input (mean value ± SEM, $n = 3$). (*C*) Protein levels of E4F1, and of the loading control Tata binding protein (TBP), determined by immunoblotting of total protein extracts prepared from *E4f1*$^{KO}$, and control tMEFs. (*D*) mRNA levels of *Dlat*, *Dld*, *Slc25a19*, *Brp44l*/*Mpc1*, *Pdpr*, and of two control genes (*CS* and *Pdha1*) determined by RT-qPCR analysis in *E4f1*$^{KO}$ and control tMEFs. Histobars represent the mean value ± SEM ($n = 6$). ***$P < 0.001$; **$P < 0.01$; *$P < 0.05$; ns, not significant.

1 (E4F1). Initially identified as a cellular target of the E1A viral oncoprotein (16), E4F1 was then described as a physical interactor of several tumor suppressors that gate cell division and survival in proliferating cells, including pRB, RASSF1A, p14$^{ARF}$, and p53 (17–21). E4F1 is essential for early embryonic mouse development (22), and for either proliferation or survival of actively dividing mammalian cells (23–25). In proliferating cells, we have recently shown that E4F1 controls genes implicated in cell-cycle checkpoints and genome surveillance, but also unexpectedly, a transcriptional program involved in mitochondria functions (24, 26). Here we further characterized this mitochondria-associated program and found that E4F1 coordinates the transcription of a set of genes involved in PDH-mediated pyruvate oxidation. Accordingly, tissue-specific inactivation of murine *E4f1* in the postmitotic and differentiated compartment of striated muscles resulted in a strong reduction of muscular PDH activity. Surprisingly, this constitutively low PDH activity did not compromise animal viability, although these animals displayed chronic lactic acidemia and endurance defects that recapitulate some clinical symptoms described in PDC-deficient patients.

## Results

**E4F1 Controls Genes Involved in PDH Activity.** We recently identified by ChIP, combined with deep sequencing (ChIP-seq), the repertoire of endogenous target DNA sites bound by E4F1 in primary and *Ha-Ras*$^{V12}$ transformed mouse embryonic fibroblasts (tMEFs) (24, 26). We completed this gene list by performing additional E4F1 ChIP-seq analyses in murine embryonic stem (ES) cells and defined a common set of promoter regions that were bound by E4F1 in these two cell types (Fig. 1*A*) (GSE57221 and GSE57228). Gene ontology analysis of E4F1 target genes revealed an unexpected enrichment for nuclear genes encoding mitochondrial proteins (24). Surprisingly, a closer analysis of this subprogram identified four genes, located on distinct chromosomes, which are directly involved in PDH function. These genes encode the E2 and E3 subunits of the PDH core enzyme (*Dlat*, *Dld*), the mitochondrial pyruvate transporter MPC1 (*Brp44l*), and the mitochondrial transporter of the PDH cofactor thiamine pyrophosphate (*Slc25a19*/*DNC*). A fifth gene, encoding the negative regulator of the PDH phosphatases (*Pdpr*) (27) was also identified as an E4F1 target gene by ChIP-seq in transformed fibroblasts, but not in ES cells (data not shown).

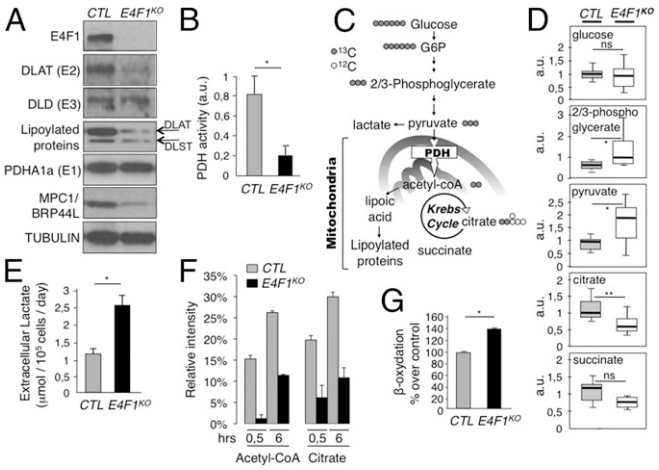


**Fig. 2.** Impaired PDH activity and deregulation of the pyruvate pathway in *E4f1*$^{KO}$ cells. (*A*) Protein levels of E4F1, DLAT, DLD, lipoylated proteins (DLAT and DLST), PDHE1a, MPC1/BRP44L, and Tubulin (loading control) determined by immunoblotting of total cell extracts prepared from *E4f1*$^{KO}$ and control (CTR) tMEFs. (*B*) PDH enzymatic activity measured in *E4f1*$^{KO}$ and CTR tMEFs. (*C*) Schematic representation of the pyruvate–AcCoA pathway. (*D*) Relative levels of several metabolites linked to the pyruvate pathway in *E4f1*$^{KO}$ and CTR tMEFs, measured by LC/MS ($n = 8$). (*E*) Extracellular lactate level in the medium of *E4f1*$^{KO}$ and CTR tMEFs. Histobars represent the mean value ± SEM ($n = 5$). (*F*) Relative abundance of M+2 isotopomers of AcCoA and citrate that derive from pyruvate oxidation as determined by LC-MS in *E4f1*$^{KO}$ and match CTR tMEFs cultured in D-[U-$^{13}$C]glucose for 30 min or 6 h (mean ± SD, experiment performed in triplicate). (*G*) Relative levels of FAO measured upon incubation of *E4f1*$^{KO}$ and CTR tMefs with $^{3}$H-palmitate (mean value ± SEM, $n = 3$). **$P < 0.01$; *$P < 0.05$; ns, not significant.

Sequence analyses revealed that these genes contained one or two bona fide E4F1 binding sites nearby their transcription start site (TSS) (Fig. 1*A*). These E4F1 direct target genes were further validated by ChIP-quantitative PCR (qPCR) experiments performed upon Cre-mediated inactivation of *E4f1* in $E4f1^{-/flox}$ tMEFs (hereafter referred to as $E4f1^{KO}$) (Fig. 1 *B* and *C*). Consistent with a role for E4F1 as a bona fide transcriptional activator for these PDH-related genes, the mRNA levels of *Dlat*, *Brp44l*/*Mpc1*, *Dld*, *Scl25A19*, and *Pdpr* decreased in $E4f1^{KO}$ cells, although to various extents (Fig. 1*D*). In contrast, the transcript levels of another PDH core component, *Pdha1*, and of the mitochondrial enzyme citrate synthase (*CS*), which were not identified as E4F1 direct target genes, did not vary upon acute *E4f1* inactivation (Fig. 1*D*). At the protein level, a strong down-regulation of DLAT and BRP44L/MPC1, and a moderate decrease of DLD were observed in $E4f1^{KO}$ cells (Fig. 2*A*). Of note, siRNA-mediated depletion of *E4f1* in fibroblasts also resulted in the down-regulation of DLAT, BRP44L/MPC1 and DLD proteins (Fig. S1*A*), confirming the role of E4F1 in the control of these genes. Taken together, our data highlight a previously undescribed function of E4F1 in the transcriptional control of genes involved in PDH activity in mammals.

***E4f1* Inactivation Results in Reduced PDH Activity and Metabolic Reprogramming.** As a direct consequence of decreased expression of PDC subunits, $E4f1^{KO}$ fibroblasts and *E4f1* siRNA-treated cells exhibited a marked decrease of PDH enzymatic activity (Fig. 2*B* and Fig. S1*B*). In E4F1-deficient cells, this reduced PDH activity should impact on pyruvate-derived mitochondrial AcCoA production, lead to accumulation of glycolytic intermediates, and induce the redirection of the glycolytic flux. We addressed this notion by performing comparative nontargeted gas chromatography/liquid chromatography-mass spectrometry (GC/LC-MS) metabolomic analyses in control and $E4f1^{KO}$ fibroblasts. As predicted, these analyses showed an accumulation of intracellular pyruvate and of its upstream precursor 2/3-phosphoglycerate (2/3PG) in $E4f1^{KO}$ cells, as well as lower levels of citrate and succinate, two intermediates of the TCA cycle (Fig. 2 *C* and *D*). E4F1-deficient cells also exhibited increased level of extracellular lactate in their culture medium (Fig. 2*E*). To further assess the PDH-dependent pyruvate oxidation pathway, we next performed stable isotope tracing experiments in control and $E4f1^{KO}$ fibroblasts cultured in presence of uniformly labeled [U-$^{13}$C]glucose. Comparative LC-MS analyses of intracellular metabolites clearly showed a strong decrease of $^{13}$C incorporation into AcCoA (M+2 isotopomer) and in its downstream metabolite, citrate (M+2 isotopomer), in $E4f1^{KO}$ cells (Fig. 2*F* and Fig. S2*A*). Of note, the relative $^{13}$C enrichment in the first glycolytic intermediates (glucose-6-phosphate, fructose-6-phosphate, fructose-1,6-biphosphate, 2/3-PG) was unaffected, suggesting that both control and $E4f1^{KO}$ fibroblasts display comparable glycolytic fluxes. Taken together, these analyses indicate that E4F1-deficiency impairs PDH activity with impacts on the pyruvate oxidation pathway (Fig. S2*A*).

Of note, we also assessed mitochondrial protein lipoylation as both a direct readout of DLAT expression and of an indirect readout of defective AcCoA production by PDH in $E4f1^{KO}$ cells (2, 28). Indeed, the precursor of lipoic acid, octanoic acid, is synthesized from mitochondrial AcCoA through fatty acid biosynthesis. Lipoic acid is then covalently attached to few proteins, for which it serves as a cofactor. At first glance, total protein lipoylation seemed to be strongly reduced in $E4f1^{KO}$ cells, as revealed by immunofluorescence (Fig. S2*B*) using an antibody that recognizes all lipoylated proteins. Although this strong decrease of total protein lipoylation likely reflects mainly DLAT protein down-regulation (the most abundant lipoylated protein), we also observed a moderate down-regulation of the lipoylation of dihydrolipoamide-S-succinyl tranferase (DLST) by immunoblotting (Fig. 2*A* and Fig. S2*C*), suggesting that the AcCoA-dependent lipoylation pathway is also partly affected in $E4f1^{KO}$ cells, and could also contribute to the phenotype of $E4f1^{KO}$. Finally, despite their low PDH activity, $E4f1^{KO}$ cells showed a moderate, but significant, decrease of intracellular ATP, as described in our previous report (see also ref. 24) (Fig. S2*D*). This moderate alteration of ATP levels suggests that alternative energetic pathways were activated in $E4f1^{KO}$ cells. Indeed, $E4f1^{KO}$ cells show signs of adaptive metabolic responses, as illustrated by increased fatty acid oxidation (FAO) (Fig. 2*G*). Accordingly, these cells were highly sensitive to the FAO inhibitor Etomoxir (Fig. S2*E*). Taken together, these data show that PDH activity and the mitochondrial pyruvate pathway are impaired in $E4f1^{KO}$ cells.

***E4f1* KO in Striated Skeletal Muscles Results in PDH Dysfunction.** We next assessed the in vivo relevance of E4F1-mediated control of this PDC transcriptional program in striated muscle, a tissue which physiological function relies on high PDH activity during exercise (10). First, we confirmed by ChIP-qPCR the recruitment of E4F1 on *Dlat*, *Dld*, *Slc25a19*, and *Brp44l*/*Mpc1* promoters in adult tibialis and

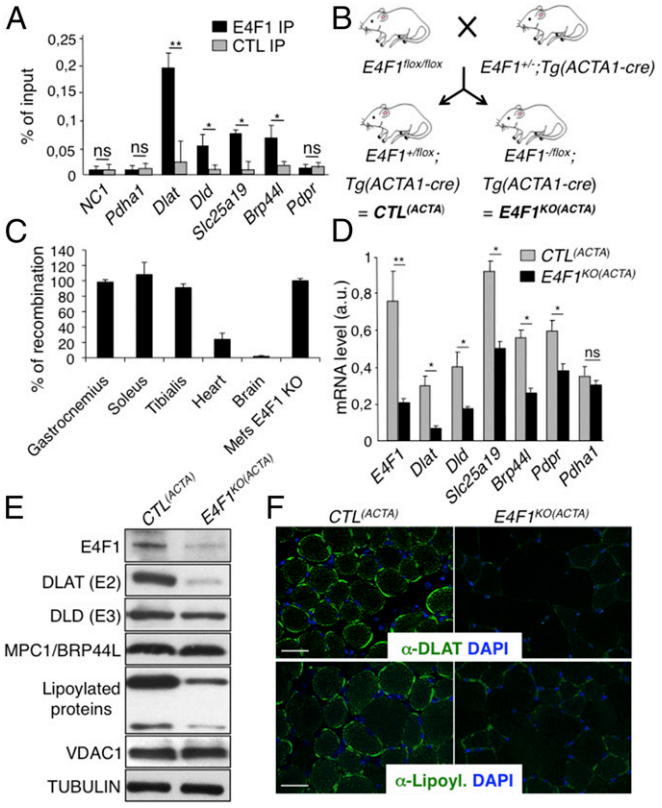


**Fig. 3.** The PDH transcriptional program controlled by E4F1 is essential to sustain PDH activity in skeletal muscles. (*A*) ChIP-qPCR experiments performed with anti-E4F1 antibody or an irrelevant control antibody on the promoter of *Dlat*, *Dld*, *Brp44l/Mpc*, *Slc25a19*, and *Pdpr* in murine striated skeletal muscles. A gene-poor noncoding region of chromosome 8 (NC1) and the *Pdha1* promoter region (TSS) were used as controls. Enrichments are represented as percentages of input (mean value ± SEM, $n = 4$). (*B*) Generation of striated skeletal muscle-specific $E4f1^{KO}$ mice. Mice harboring the *E4f1* null and flox alleles were intercrossed with Tg(*Acta1*-Cre) transgenic mice to generate $E4f1^{-/flox}$; Tg(*Acta1*-Cre) and $E4f1^{+/flox}$; Tg(*Acta1*-Cre) control littermates [$E4f1^{KO(ACTA)}$ and $CTL^{(ACTA)}$, respectively]. (*C*) Cre-mediated recombination efficiency of the *E4f1* flox allele in vivo was assessed by qPCR analysis on genomic DNA prepared from striated muscles, heart, and brain. Cre-mediated recombination in $E4f1^{flox}$ tMEFs was used to normalize (100% efficiency). Histobars represent the mean value ± SEM ($n = 3$). (*D*) mRNA levels of *Dlat*, *Dld*, *Slc25a19*, *Brp44l/Mpc1*, *Pdpr* and of a control gene (*Pdha1*) in striated muscles prepared from 16-wk-old $E4f1^{KO(ACTA)}$ and $CTL^{(ACTA)}$ animals. Histobars represent the mean value ± SEM ($n = 5$) measured by RT-qPCR. (*E*) Protein levels of E4F1, DLAT, DLD, MPC1/BRP44L, lipoylated proteins, VDAC and Tubulin (loading control) determined by immunoblotting of total cell extracts prepared from the same animals than in *D*. (*F*) Immunofluorescence analysis of DLAT (*Upper*) and lipoylated proteins (*Lower*) in muscle sections prepared from $E4f1^{KO(ACTA)}$ and $CTL^{(ACTA)}$ animals. (Scale bars, 200 μm.) $^{**}P < 0.01$; $^{*}P < 0.05$; ns, not significant.

gastrocnemius muscles of resting mice, indicating that E4F1–PDH program also exists in adult muscle cells (Fig. 3*A* and Fig. S3*A*). Then, we inactivated *E4f1* in vivo in striated muscles by crossing $E4f1^{-/flox}$ mice with *Acta1-Cre* transgenic (Tg) mice that express the Cre recombinase under the control of the skeletal α-actin promoter [hereafter referred to as Tg(*Acta1-Cre*)] (Fig. 3*B*) (29). We verified the efficiency and the tissular specificity of Cre-driven recombination of the $E4f1^{flox}$ allele in $E4f1^{-/flox}$; Tg(*Acta1-Cre*) and $E4f1^{+/flox}$; Tg(*Acta1-Cre*) control littermates [hereafter referred to as $CTL^{(ACTA)}$ and $E4f1^{KO(ACTA)}$, respectively]. Cre-driven inactivation of the $E4f1^{flox}$ allele was largely restricted to striated skeletal muscles, as shown by the strong reduction of *E4f1* mRNA and protein levels in gastrocnemius of adult $E4f1^{KO(ACTA)}$ mice (Fig. 3 *D* and *E*). Although limited Cre-mediated recombination (20% efficiency) was also detected in heart (Fig. 3*C*), this did not impair significantly the cardiac mRNA level of *E4f1* when assessed at the whole tissue level (Fig. S3*B*). $E4f1^{KO(ACTA)}$ mice were healthy and viable, and detailed anatomo-pathological analyses of skeletal muscles at 16 wk of age revealed neither major histological alterations nor significant differences in the number and size of muscle fibers compared with control littermates (Fig. S4 *A*, *B*, and *D*). Accordingly, mRNA levels of muscular differentiation markers and inducers such as *Mif6*, *Mef2c*, *MyoD*, and *Myogenin* were similar in adult striated muscles of 16-wk-old $E4f1^{KO(ACTA)}$ and control mice (Fig. S4*E*). However, alterations resembling degenerative to necrotizing and diffuse myopathy were gradually detected in older animals. Thus, H&E staining of striated muscle sections prepared from 18-mo-old animals showed that *E4f1 KO* led to myophagocytosis, hypercontracted fibers, centralized regenerative fibers, immune cell infiltration, and the presence of adipocytes (Fig. S4*A*). These data suggest that in the long term, E4F1 deficiency results in skeletal muscle disorganization and histological alterations.

Next, we evaluated the consequences of *E4f1* inactivation in vivo on this PDH transcriptional program. In skeletal, but not in cardiac $E4f1^{KO}$ muscles, mRNA, and protein levels of *Dlat* were strongly altered, whereas the mRNA level of *Pdha1*, used as control, remained unchanged (Fig. 3 *D*–*F* and Fig. S3*B*). Expression of *Brp44l*, *Slc25a19*, and *Dld* was also slightly decreased at the mRNA level (Fig. 3*D*), although to a lesser extent than *Dlat*. As in $E4f1^{KO}$ fibroblasts (tMEFs) in culture, protein lipoylation was also markedly decreased in $E4f1^{KO}$ muscles, as shown by immunoblotting on proteins extracts and immunostaining of tissue sections (Fig. 3 *E* and *F*). Impaired expression of these PDC components in $E4f1^{KO}$ muscles resulted in 80–90% reduction of PDH enzymatic activity in gastrocnemius, as measured by two independent methods (Fig. 4 *A* and *B* and Fig. S3*D*). $E4f1^{KO(ACTA)}$ mice also exhibited increased level of circulating ketone bodies, suggesting that $E4f1^{KO}$ muscles activated FAO as in $E4f1^{KO}$ tMEFs (Fig. 4*C*). Of note, DLAT expression and PDH activity were also strongly down-regulated in extensor digitorum longus and soleus striated muscles isolated from $E4f1^{KO(ACTA)}$ mice, indicating that both red and white muscle fibers are equally affected by E4F1-deficiency (Fig. S5 *A* and *B*). Consistent with the absence of depletion of *E4f1* mRNA in cardiac tissue in this animal model (Fig. S3*B*), no significant difference in PDH activity was detected in the heart of $E4f1^{KO(ACTA)}$ mice (Fig. S3*C*). These data show that the E4F1–PDH connection is critical for the pyruvate-AcCoA metabolic pathway in adult striated skeletal muscles, confirming its biological relevance in vivo.

***E4f1* Inactivation in Skeletal Muscles Results in Lactate Acidosis and Muscular Endurance Defects.** Although *E4f1*-deficient muscles display a strong reduction of basal PDH activity, 16-wk-old $E4f1^{KO(ACTA)}$ mice did not show spontaneous locomotor deficiency in normal housing conditions, as quantified by infrared light beam interruption in cages (Fig. S4*C*). This surprising result indicates that a low muscular PDH activity (10–20% of normal levels) (Fig. 4 *A* and *B*) is sufficient to sustain basal locomotor activity and viability. PDH activity has been documented to increase in skeletal muscles during high-intensity exercise and to contribute to muscular endurance (10).

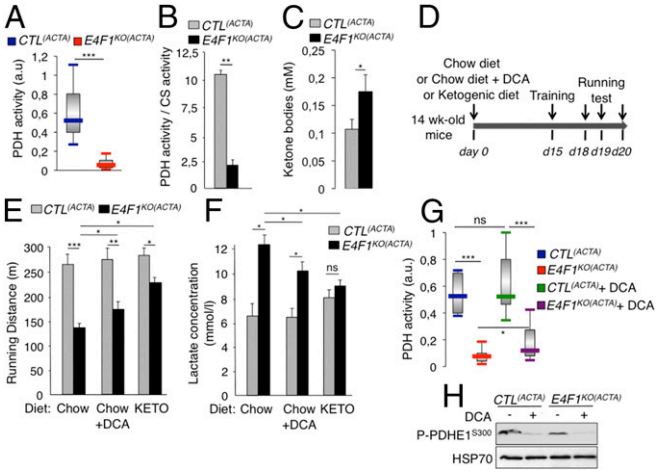


**Fig. 4.** *E4f1* inactivation in skeletal muscles results in reduced PDH activity, chronic lactate acidosis and reduced muscular endurance. (*A* and *B*) PDH activity measured in protein extracts prepared from gastrocnemius of resting 16-wk-old $E4f1^{KO(ACTA)}$ animals and $CTL^{(ACTA)}$ littermates using two different methods, DipStick Assay (*A*) or [$^{14}$C]-Pyruvate oxidation assay (*B*). CS enzymatic activity that does not vary (Fig. S3*D*) was used to normalize PDH activity in *B*. Histobars represent the mean value ± SEM of $n = 5$ (*A*) and $n = 2$ (*B*) independent experiments. (*C*) Ketone bodies level in serum of $E4f1^{KO(ACTA)}$ and $CTL^{(ACTA)}$ males. (*D*) Schematic representation of the experimental design to measure the impact of *E4f1* inactivation on physical endurance. A shift from a chow to a ketogenic (KETO) diet or addition of DCA in drinking water was done 2 wk before the first training session. (*E*) Locomotor performance (running distance before exhaustion) of 16-wk-old $E4f1^{KO(ACTA)}$ and $CTL^{(ACTA)}$ animals under chow or KETO diets, or after administration of DCA, was evaluated using forced treadmill running. Histobars represent the mean value ± SEM of three independent measurements for each animal ($n = 8$ males per group). (*F*) Lactate level (serum) of $E4f1^{KO(ACTA)}$ and $CTL^{(ACTA)}$ males under chow or ketogenic diets, or after administration of DCA, measured after running. Histobars represent the mean value ± SEM ($n = 8$ males per group). (*G*) PDH activity was measured after running in protein extracts from striated muscles of $E4f1^{KO(ACTA)}$ and $CTL^{(ACTA)}$ males, in the presence or absence of DCA. Histobars represent the mean value ± SEM ($n = 5$). (*H*) Phosphorylation level of serine 300 of PDHE1 assessed by immunoblotting of total protein extracts from gastrocnemius of $E4f1^{KO(ACTA)}$ and $CTL^{(ACTA)}$ animals, in the absence or presence of DCA. HSP70 protein was used as loading control. $^{***}P < 0.001$; $^{**}P < 0.01$; $^{*}P < 0.05$; ns, not significant.

Therefore, we hypothesized that the residual PDH activity in muscles of $E4f1^{KO(ACTA)}$ mice might not be sufficient to support the energetic demand that occurs during an acute and high exercise workload. Locomotor activity of control and $E4f1^{KO(ACTA)}$ adult mice was assessed upon forced treadmill running (Fig. 4*D*). Although PDH activity increased in all animals in this experimental setting, it remained much lower in $E4f1^{KO(ACTA)}$ mice relative to control littermates (Fig. 4*G*). Accordingly, $E4f1^{KO(ACTA)}$ animals displayed a marked decrease of their physical endurance, as documented by a twofold reduction of their running performance [total running distance (Fig. 4*E*) and time to exhaustion (Fig. S6*A*)].

Because PDH deficiency results in chronic lactic acidemia in patients, we measured lactate levels in the serum of $E4f1^{KO(ACTA)}$ and control mice. $E4f1^{KO(ACTA)}$ animals exhibited increased lactate levels relative to controls under normal housing conditions and regular chow diet (Fig. S6*B*). Lactic acidemia was further exacerbated upon acute exercise (Fig. 4*F*). Importantly, 16-wk-old $E4f1^{KO(ACTA)}$ mice showed no apparent alterations of glucose homeostasis, as assessed by insulin- and glucose-tolerance tests (Fig. S6 *C* and *D*), glucose uptake, and expression of the glucose transporter GLUT1 (Fig. S6 *E* and *F*). Collectively, our data show that $E4f1^{KO(ACTA)}$ mice display phenotypes that recapitulate some clinical symptoms observed in PDC-deficient patients, including lactic acidemia and exercise intolerance (11, 30).

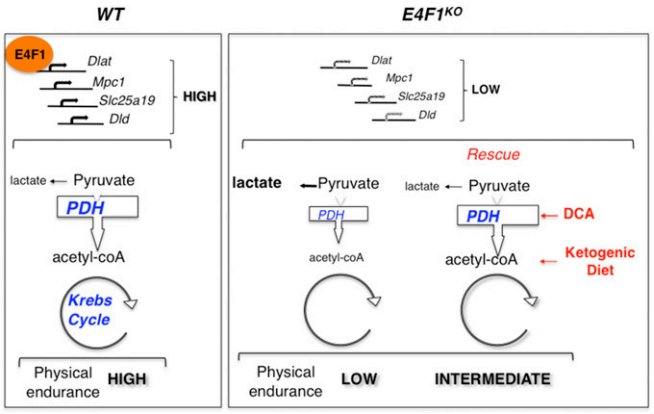


**Fig. 5.** Schematic representation of E4F1-mediated effects on pyruvate metabolism. E4F1 protein controls transcription of a set of genes encoding core components or regulators of the PDC. E4F1 deficiency results in impaired PDH activity and redirection of the glycolytic flux toward lactate production. Mice with *E4f1*-deficient skeletal muscles exhibit muscular endurance defects and chronic lactate acidemia. Like in PDC-deficient patients, these defects are partly improved by ketogenic diet (KETO) or by treatment with a PDH activator, DCA.

**Muscular defects of $E4f1^{KO(ACTA)}$ Mice Are Rescued upon Pharmacological Reactivation of PDH or Under a Ketogenic Diet.** We next evaluated in $E4f1^{KO(ACTA)}$ mice the impact of DCA treatment and of a ketogenic diet, two therapies that are included in the standard care of many PDC-deficient patients. $E4f1^{KO(ACTA)}$ and control animals were treated for 2 wk with the PDK-inhibitor DCA before evaluating their endurance capacity (Fig. 4*D*). This treatment reduced the inhibitory phosphorylation of the PDHE1 subunit on serine 300 (Fig. 4*H*), resulting in a moderate but significant increase of muscular PDH activity in $E4f1^{KO(ACTA)}$ mice (Fig. 4*G*). This finding suggested that the residual pool of PDC in $E4f1^{KO}$ muscles was amenable to DCA treatment. Remarkably, as in PDC-deficient patients, this treatment improved the physical endurance and reduced the lactic acidemia of $E4f1^{KO(ACTA)}$ mice exposed to intense treadmill exercise (Fig. 4 *E* and *F* and Fig. S6*A*).

Ketogenic diet provides an alternative source of energy and AcCoA through increased FAO that partly improve physical fitness and lactate acidemia in PDC-deficient patients. Importantly, its efficacy was confirmed in zebrafish models with mutations in *Dlat* or *Pdhb* (31, 32). Accordingly, feeding $E4f1^{KO(ACTA)}$ mice with a ketogenic diet (Fig. 4*D*) significantly improved their running capacity and normalized their blood lactate level (Figs. 4 *E* and *F* and Fig. S6*A*). Of note, beneficial effects of these two treatments on $E4f1^{KO(ACTA)}$ mice were clear but remained partial, a situation also observed in PDC-deficient patients (14). Collectively, these rescue experiments confirm that the muscular phenotypes observed in E4F1-deficient animals result from PDH deficiency (Fig. 5).

## Discussion

Here, we describe a level of regulation of PDH in mammals implicating the E4F1 transcription factor. To characterize its role in PDH-regulation, we developed a skeletal muscle-specific *E4f1* KO mouse model, the phenotypes of which recapitulate some clinical symptoms observed in PDC-deficient patients.

In mammals, the control of PDC activity has been mainly attributed to posttranslational modifications of its subunits by PDKs and PDPs. Its control at the transcriptional level has been far less investigated and mainly concerns the regulation of individual *Pdk* genes by multiple transcription factors, including *Foxo1/3a* (33), *Hif1a* (34), *or p53* (35). Nevertheless, in more primitive organisms, it was demonstrated that genes coding for other regulators, but also for core PDC components, are coregulated and organized in regulons or operons. Thus, in *E. coli*, the *aceE*/E1, the *aceF*/E2, and *IpdA*/E3 genes form a single operon that also includes the transcriptional regulator of this operon *PdpR* (7). In *C. albicans*, the Gal4p transcriptional regulator controls the expression of the five main components of the PDC complex, including the *Pda1*/E1, *Pdb1*/E1, *Dlat1*/E2, *Lpd1*/E3, and *Pdx1* subunits (8). Our data reveal that such a coordinated transcriptional program, important for PDH-mediated pyruvate oxidation, also exists in mammals. Composed of at least four genes—*Dlat/E2*, *Dld/E3*, *Brp44l/MPC1*, and *Slc25a19*—this program is controlled by E4F1, a sequence-specific transcription factor bound nearby the TSS of these genes.

This E4F1-controlled transcription program is a main contributor of the total PDH activity, as demonstrated by the impact of conditional gene targeting of *E4f1* in proliferating cells and in postmitotic differentiated muscular cells that resulted in a 80–90% reduction of the basal PDH activity. Surprisingly, we show that, despite their very weak muscular PDH activity, animals lacking E4F1 in their striated muscles were viable and displayed normal basal locomotor activity, at least in normal housing conditions. Nevertheless, these animals exhibited lactic acidemia and severe exercise intolerance that were partly rescued by the pharmacological reactivation of the remaining pool of PDC by DCA, or by shunting the need for PDH activity by promoting FAO using a ketogenic diet. Our histological analyses indicate that although *E4f1* inactivation did not result in major disorganization of this tissue in young animals, long-term PDH-deficiency led to a degenerative muscular myopathy in older animals. So far, such clinical symptoms have not been described in PDC patients, likely because most of these patients do not live long enough to develop myopathies. On the other hand, it is commonly described that these patients often exhibit epileptic seizures and microcephalies. These symptoms were not observed in our muscle-specific $E4f1^{KO}$ mice, despite these animals displayed chronic lactic acidemia. This finding questions the origin of the neurological manifestations observed in PDC patients and suggests that the latter symptoms do not result solely from chronic systemic lactic acidemia, but could also arise from multiple brain-specific metabolic alterations. Tissue-specific inactivation of *E4f1* in the central nervous system may provide a definitive answer to this clinically relevant question.

Strikingly, recent genetic studies designed to identify new mutated genes involved in unsolved cases of primary mitochondrial human disorders, led to the identification of a homozygous nonsynonymous mutation in the *E4F1* gene of a patient showing reduced PDH complex activity, muscular defects, and lactate acidemia (36). This first indication that the E4F1-controlled program could be deregulated in a pathological situation provides an exciting clinical perspective to the present work. Indeed, our $E4f1^{KO(ACTA)}$ animal models display phenotypes that recapitulate some clinical symptoms observed in this PDC-deficient patient. Thus, these animals could represent potential models for preclinical studies aiming at testing new therapeutic strategies to improve the consequences of PDH deficiency.

Furthermore, it should be noted that missense mutations in the E4F1-target genes *Dlat*, *Dld*, *Brp44l*, and *Slc25a19* have been identified in several congenital metabolic disorders associated with reduced PDH activity and alteration of the pyruvate oxidation pathway. These disorders include PDC deficiency, lipoamide dehydrogenase deficiency, or Amish lethal microcephaly syndromes (3, 11, 13). It is also worth noting that complete KO mouse models for *Pdha1*, *Dld*, *Slc25a19*, as well as for *E4f1*, all show severe developmental defects and lethality during early embryonic development (4, 22, 37–39). This finding raises interesting questions about the importance of the E4F1-controlled PDH-program during embryogenesis and beyond, about the poorly characterized metabolic rewiring of the pyruvate pathway that may occur during development.

Altogether, our data highlight the role of E4F1 in PDH-dependent metabolic homeostasis and pave the way for new studies on the physiological rewiring of the pyruvate pathway. This work should also stimulate new research aiming at exploring the role of nuclear transcription factors in unsolved cases of mitochondrial diseases.

## Experimental Procedures

**Accession Numbers.** The full series of data, including expression arrays and ChIP-Seq data reported in this paper were deposited on the Gene Expression Omnibus (GEO) dataset repository (see GEO SuperSeries GSE57242 and GSE57221) (24, 26). E4F1 binding regions were defined by combining bioinformatic toolboxes

provided by CisGenome and Qeseq software systems. Detailed protocols, bioinformatic tools and primers used for ChIp-seq and ChIP-qPCR validations were as previously described (24, 26) and detailed in *SI Experimental Procedures*.

**Mouse Models and Experimental Treatment.** *E4f1*$^{-/+}$, *E4f1*$^{+/flox}$, and *E4f1*$^{-/flox}$ mice (22, 40) were intercrossed with *ActaCre* mice to obtain *E4f1*$^{+/flox}$*; ActaCre* and *E4f1*$^{-/flox}$*; ActaCre* compound mice on a mixed 129Sv/J/DBA/C57BL/6 background. Phenotypic characterization of compound *E4f1*$^{KO(ACTA)}$ and *CTL*$^{(ACTA)}$ mice was performed on 16-wk-old or 18-mo-old littermates. Mice were housed in a pathogen-free barrier facility in accordance with the ethic Committee for Animal Welfare (Comité d'Ethique en Experimenttion Animal - Languedoc Rossillon, CEEA-LR-12116). Mice were maintained under chow diet (A03, Safe; i.e., 22 kcal% protein, 65 kcal% carbohydrate, and 13 kcal% fat) in the presence or absence of DCA in the drinking water (added to the drinking water for 2 wk at a final concentration of 2 g/L), or were fed with a ketogenic diet (F3666, Bio-Serv; 5kcal% protein, 2kcal% carbohydrate, and 93kcal% fat) for 2 wk before assessing their physical performances, as detailed in *SI Experimental Procedures*.

**PDH Activity and Lactate Measurements, Metabolomics.** Two different protocols were used in parallel to measure PDH activity in protein extracts prepared from cells or muscles (gastrocnemius and heart). PDH activity DipStick Assay Kit (ab109882, Abcam) was used on cell (25 μg) or muscle (5 μg) extracts prepared according to the manufacturer's protocol, and quantified by ImageJ. PDH enzymatic activity was also assessed by measuring the release of $^{14}CO_2$ after incubation of protein extracts (1 mg of protein per milliliter) with [1-$^{14}$C] pyruvate, as previously described and detailed in *SI Experimental Procedures* (41). To determine the concentration of glucose, 2/3PG, pyruvate, citrate, and succinate in *E4f1* WT and KO tMEFs, extracts were prepared from $2 \times 10^7$ cells and analyzed by GC/MS and LC/MS/MS platforms (Metabolon). Eight independent samples were analyzed for each cell lines. Lactate production by cells was measured in culture medium using a L-Lactate Assay Kit (Eton Bioscience). Lactate and ketone bodies concentration in blood were measured using a lactometer (EKF Diagnostics) and β-ketone strips (Optium, Abbott), respectively.

**Statistical Analysis.** Unpaired Student's *t* test was used in all analyses. Statistical significance was expressed as follows: $*P < 0.05$, $**P < 0.01$, $***P < 0.001$.

**Supplemental Materials and Methods.** Experimental procedures relative to genotyping of animal models, generation of cells, RT-qPCR analyses, siRNA-mediated E4f1-depletion, immunoblotting, immunohistochemistry, and immunofluorescence assays, measurement of FAO, and stable isotope tracing, insulin- and glucose-tolerance tests, and in vivo glucose uptake, are described in *SI Experimental Procedures*.

**ACKNOWLEDGMENTS.** This work was supported by grants from the Ligue Nationale Contre le Cancer (LNCC, équipes labelisées 2011 (to C.S.) and 2016 (to L.L.C.); Agence Nationale pour la Recherche Grants SVSE2-YinE4F1Yang2 and MetaboCycle2 (to C.S. and L.L.C.); grants from the Fondation ARC and from the Canceropole Grand Sud Ouest (to G.R.); institutional support from INSERM (L.L.C. and C.S.), the Site de Recherche Intégrée sur le Cancer Montpellier Cancer Grant INCa-DGOS-Inserm 6045 (to C.S.) and CNRS (C.S.); fellowships from LNCC (to T.H. and M.L.); fellowships financed on the Agence Nationale pour la Recherche Grants JCJC-0014-01 and SVSE2-YinE4F1Yang2 (to O.K. and H.D.); LabEx EpiGenMed ANR-10-LABX-12-01 (to B.S.); and the technical support of Montpellier Rio Imaging (MRI), Genomics (MGX), Metamus and Animal (RAM) facilities.

1. Patel MS, Nemeria NS, Furey W, Jordan F (2014) The pyruvate dehydrogenase complexes: Structure-based function and regulation. *J Biol Chem* 289(24):16615–16623.
2. Herzig S, et al. (2012) Identification and functional expression of the mitochondrial pyruvate carrier. *Science* 337(6090):93–96.
3. Bricker DK, et al. (2012) A mitochondrial pyruvate carrier required for pyruvate uptake in yeast, *Drosophila*, and humans. *Science* 337(6090):96–100.
4. Lindhurst MJ, et al. (2006) Knockout of Slc25a19 causes mitochondrial thiamine pyrophosphate depletion, embryonic lethality, CNS malformations, and anemia. *Proc Natl Acad Sci USA* 103(43):15927–15932.
5. Patel MS, Korotchkina LG (2006) Regulation of the pyruvate dehydrogenase complex. *Biochem Soc Trans* 34(Pt 2):217–222.
6. Mathias RA, et al. (2014) Sirtuin 4 is a lipoamidase regulating pyruvate dehydrogenase complex activity. *Cell* 159(7):1615–1625.
7. Ogasawara H, Ishida Y, Yamada K, Yamamoto K, Ishihama A (2007) PdhR (pyruvate dehydrogenase complex regulator) controls the respiratory electron transport system in *Escherichia coli*. *J Bacteriol* 189(15):5534–5541.
8. Askew C, et al. (2009) Transcriptional regulation of carbohydrate metabolism in the human pathogen *Candida albicans*. *PLoS Pathog* 5(10):e1000612.
9. Rajagopalan KN, et al. (2015) Metabolic plasticity maintains proliferation in pyruvate dehydrogenase deficient cells. *Cancer Metab* 3:7.
10. Peters SJ (2003) Regulation of PDH activity and isoform expression: Diet and exercise. *Biochem Soc Trans* 31(Pt 6):1274–1280.
11. Patel KP, O'Brien TW, Subramony SH, Shuster J, Stacpoole PW (2012) The spectrum of pyruvate dehydrogenase complex deficiency: Clinical, biochemical and genetic features in 371 patients. *Mol Genet Metab* 106(3):385–394.
12. Maj MC, et al. (2005) Pyruvate dehydrogenase phosphatase deficiency: identification of the first mutation in two brothers and restoration of activity by protein complementation. *J Clin Endocrinol Metab* 90(7):4101–4107.
13. Rosenberg MJ, et al. (2002) Mutant deoxynucleotide carrier is associated with congenital microcephaly. *Nat Genet* 32(1):175–179.
14. Abdelmalak M, et al. (2013) Long-term safety of dichloroacetate in congenital lactic acidosis. *Mol Genet Metab* 109(2):139–143.
15. Ferriero R, et al. (2013) Phenylbutyrate therapy for pyruvate dehydrogenase complex deficiency and lactic acidosis. *Sci Transl Med* 5(175):175ra31.
16. Raychaudhuri P, Rooney R, Nevins JR (1987) Identification of an E1A-inducible cellular factor that interacts with regulatory sequences within the adenovirus E4 promoter. *EMBO J* 6(13):4073–4081.
17. Rizos H, et al. (2003) Association of p14ARF with the p120E4F transcriptional repressor enhances cell cycle inhibition. *J Biol Chem* 278(7):4981–4989.
18. Le Cam L, et al. (2006) E4F1 is an atypical ubiquitin ligase that modulates p53 effector functions independently of degradation. *Cell* 127(4):775–788.
19. Fenton SL, et al. (2004) Identification of the E1A-regulated transcription factor p120 E4F as an interacting partner of the RASSF1A candidate tumor suppressor gene. *Cancer Res* 64(1):102–107.
20. Sandy P, et al. (2000) p53 is involved in the p120E4F-mediated growth arrest. *Oncogene* 19(2):188–199.
21. Fajas L, et al. (2000) pRB binds to and modulates the transrepressing activity of the E1A-regulated transcription factor p120E4F. *Proc Natl Acad Sci USA* 97(14):7738–7743.
22. Le Cam L, Lacroix M, Ciemerych MA, Sardet C, Sicinski P (2004) The E4F protein is required for mitotic progression during embryonic cell cycles. *Mol Cell Biol* 24(14):6467–6475.
23. Hatchi E, et al. (2011) E4F1 deficiency results in oxidative stress-mediated cell death of leukemic cells. *J Exp Med* 208(7):1403–1417.
24. Rodier G, et al. (2015) The transcription factor E4F1 coordinates CHK1-dependent checkpoint and mitochondrial functions. *Cell Reports* 11(2):220–233.
25. Grote D, et al. (2015) E4F1 is a master regulator of CHK1-mediated functions. *Cell Reports* 11(2):210–219.
26. Houlès T, Rodier G, Le Cam L, Sardet C, Kirsh O (2015) Description of an optimized ChIP-seq analysis pipeline dedicated to genome wide identification of E4F1 binding sites in primary and transformed MEFs. *Genom Data* 5:368–370.
27. Yan J, Lawson JE, Reed LJ (1996) Role of the regulatory subunit of bovine pyruvate dehydrogenase phosphatase. *Proc Natl Acad Sci USA* 93(10):4953–4956.
28. Lawson JE, Niu XD, Reed LJ (2001) Functional analysis of the domains of dihydrolipoamide acetyltransferase from *Saccharomyces cerevisiae*. *Biochemistry* 30(47):11249–11254.
29. Miniou P, et al. (1999) Gene targeting restricted to mouse striated muscle lineage. *Nucleic Acids Res* 27(19):e27.
30. Cameron JM, et al. (2007) Identification of a canine model of pyruvate dehydrogenase phosphatase 1 deficiency. *Mol Genet Metab* 90(1):15–23.
31. Taylor MR, Hurley JB, Van Epps HA, Brockerhoff SE (2004) A zebrafish model for pyruvate dehydrogenase deficiency: Rescue of neurological dysfunction and embryonic lethality using a ketogenic diet. *Proc Natl Acad Sci USA* 101(13):4584–4589.
32. Maurer CM, Schönthaler HB, Mueller KP, Neuhauss SCF (2010) Distinct retinal deficits in a zebrafish pyruvate dehydrogenase-deficient mutant. *J Neurosci* 30(36):11962–11972.
33. Kwon H-S, Huang B, Unterman TG, Harris RA (2004) Protein kinase B-alpha inhibits human pyruvate dehydrogenase kinase-4 gene induction by dexamethasone through inactivation of FOXO transcription factors. *Diabetes* 53(4):899–910.
34. Kim J-W, Tchernyshyov I, Semenza GL, Dang CV (2006) HIF-1-mediated expression of pyruvate dehydrogenase kinase: A metabolic switch required for cellular adaptation to hypoxia. *Cell Metab* 3(3):177–185.
35. Contractor T, Harris CR (2012) p53 negatively regulates transcription of the pyruvate dehydrogenase kinase Pdk2. *Cancer Res* 72(2):560–567.
36. Legati A, et al. (2016) New genes and pathomechanisms in mitochondrial disorders unraveled by NGS technologies. *Biochim Biophys Acta* 1857(8):1326–1335.
37. Johnson MT, et al. (2001) Inactivation of the murine pyruvate dehydrogenase (Pdha1) gene and its effect on early embryonic development. *Mol Genet Metab* 74(3):293–302.
38. Johnson MT, Yang HS, Magnuson T, Patel MS (1997) Targeted disruption of the murine dihydrolipoamide dehydrogenase gene (Dld) results in perigastrulation lethality. *Proc Natl Acad Sci USA* 94(26):14512–14517.
39. Pliss L, et al. (2013) Cerebral developmental abnormalities in a mouse with systemic pyruvate dehydrogenase deficiency. *PLoS One* 8(6):e67473.
40. Lacroix M, et al. (2010) Transcription factor E4F1 is essential for epidermal stem cell maintenance and skin homeostasis. *Proc Natl Acad Sci USA* 107(49):21076–21081.
41. Brivet M, et al. (2003) Impaired mitochondrial pyruvate importation in a patient and a fetus at risk. *Mol Genet Metab* 78(3):186–192.
42. Silver DP, Livingston DM (2001) Self-excising retroviral vectors encoding the Cre recombinase overcome Cre-mediated cellular toxicity. *Mol Cell* 8(1):233–243.
43. Pessemesse L, et al. (2012) Depletion of the p43 mitochondrial T3 receptor in mice affects skeletal muscle development and activity. *FASEB J* 26(2):748–756.
44. Martano G, et al. (2015) Fast sampling method for mammalian cell metabolic analyses using liquid chromatography-mass spectrometry. *Nat Protoc* 10(1):1–11.